ELSEVIER

1 January 1997

OPTICS COMMUNICATIONS

Optics Communications 133 (1997) 565–577

Full length article

Nonlinear dynamics in the generalized Lorenz-Haken model

Guido H.M. van Tartwijk [1], Govind P. Agrawal

The Institute of Optics, University of Rochester, Rochester, NY 14627, USA

Received 15 April 1996; revised version received 5 September 1996; accepted 6 September 1996

Abstract

We introduce a generalized form of the Lorenz-Haken equations governing single-mode laser dynamics. Our generalization allows for asymmetric gain as well as inhomogeneous broadening through two additional parameters. By analyzing the steady states and their stability of this new set of equations we find that a second (instability) threshold exists in a large region of parameter space, while the traditional Lorenz-Haken equations show no such threshold. Examples of dynamic evolution in the region beyond the second threshold are given as a function of the two new parameters. Our generalized model is a somewhat simplified version of a recently proposed model for describing ultrafast dynamics of single-mode semiconductor lasers, and we discuss the possible implications of our results for such lasers.

PACS: 05.45.+b; 42.65.Sf; 42.60.Mi; 42.55.Px

1. Introduction

Nonlinear laser dynamics, following the footsteps of the more traditional field of hydrodynamics, has attracted considerable attention since its beginning in 1975. In that year, Haken showed the isomorphic nature of the well-known hydrodynamical Lorenz equations and the Maxwell-Bloch equations governing the dynamics of a homogeneously broadened resonant two-level system [1,2]. The concept of chaos was introduced in optics, and by now most scientists are aware of its usefulness: one learns more from the instabilities of a system than from its stable fixed points.

Single-mode lasers are often classified into three classes, introduced by Arecchi et al. [3,4]. The classification is based on the relative magnitudes of the three relaxation times associated with the optical field τ_E, the induced polarization τ_P, and the inversion τ_N. The dynamics of class-A lasers are dictated by the optical field; the induced polarization as well as the inversion can be adiabatically eliminated, since their relaxation times are much smaller than that of the optical field. For class-B lasers, only the induced polarization is adiabatically eliminated, while for class-C lasers all three quantities have comparable relaxation times.

Class-C lasers (e.g. He-Xe lasers) can become chaotic by themselves when pumped hard enough, but only when they satisfy the bad-cavity condition

$$\sigma > b + 1, \tag{1}$$

where $\sigma = \tau_P/\tau_E$ and $b = \tau_P/\tau_N$. The smallest pump at which the continuous-wave (CW) output becomes unstable is called the second threshold, the first threshold being the pump at which CW lasing starts. For lasers that do not satisfy the bad-cavity condition, the second threshold is said to be at infinity.

Both class-A and class-B lasers need additional degrees of freedom (externally provided through phe-

[1] Fax: (716)-244-4936; E-mail: guido@optics.rochester.edu.

PII S0030-4018(96)00589-5

nomena such as pump modulation, optical injection, and electrical or optical delayed feedback) to exhibit chaos [4]. Because of the impractically of high values of the second threshold of class-C lasers (at 21 times lasing threshold for a laser with $\sigma = 3$ and $b = 1$), recent attention has focused on class-B lasers operated under (or a combination of) pump modulation, optical injection, and optical feedback. An example of a class-B laser is a single-mode semiconductor laser, provided the photon lifetime $\tau_{ph} \equiv \tau_E/2$ is well above 1 ps. In the presence of external optical feedback, single-mode semiconductor lasers show a wealth of nonlinear dynamics that have attracted researchers since the early 1980s (for some recent papers, see Refs. [5–7]).

The classification scheme of single-mode lasers is based on a homogeneously broadened two-level system (with a symmetric Lorentzian gain profile), whose dynamics are governed by the Lorenz-Haken equations. Graham and Cho [8] showed that for inhomogeneously broadened two-level systems, an infinite hierarchy of Lorenz-Haken models exists, successive orders increasing in accuracy and complexity. They showed analytically that the second threshold for such systems is always reduced compared with the homogeneously broadened case. In this paper we introduce the generalized Lorenz-Haken equations, in which two additional parameters account for the asymmetry of the gain profile and inhomogeneous broadening. The "classical" Lorenz-Haken equations, including its detuned version, represent special cases of this new set of equations. These generalized equations were recently derived in the context of single-mode semiconductor laser dynamics [9].

In Section 2 we introduce the model and discuss its relation to existing laser models. In Section 3 we analyze its fixed points and their stability, with special attention to the location of the second threshold, and in Section 4 we give some examples of dynamics beyond the second threshold. In Section 5, we discuss the possible application of our model to a single-mode semiconductor laser. We show that the generalized Lorenz-Haken equations are a somewhat simplified form of a recently derived model for ultrafast semiconductor laser dynamics. We find that a second threshold exists for semiconductor lasers, which may lead to self-pulsating behavior at high frequencies. We discuss how the second threshold can be lowered in practice.

2. Generalized Lorenz-Haken model

In this section we introduce and discuss the properties of a new set of equations that can be regarded as a generalization of the well-known Lorenz-Haken equations [2,10]. In the standard notation of Ref. [10], the new equations take the form:

$$\frac{dx}{dt} = -\sigma(x - y), \tag{2}$$

$$\frac{dy}{dt} = -(1 + i\theta)\left[y - (1 - i\alpha)(r - z)x\right], \tag{3}$$

$$\frac{dz}{dt} = -bz + \mathrm{Re}(x^* y). \tag{4}$$

In the optical language, x is proportional to the electric field, y is proportional to the induced macroscopic polarization, $(r - z)$ denotes the inversion, $\sigma = \tau_P/\tau_E$, $b = \tau_P/\tau_N$, and time t is normalized to the polarization relaxation time τ_P. The two parameters α and θ are new: α governs the coupling between amplitude and phase variations and has its origin in the asymmetry of the gain profile. In the semiconductor laser literature, α is known as the linewidth enhancement factor [11]. The effective detuning θ has its origin in the inhomogeneous broadening of the resonance. The parameter r is a measure for the pump strength and is normalized such that the first (lasing) threshold occurs at $r = 1$ when $\alpha = \theta = 0$. Note that, since r is a constant, both z and $r - z$ are proportional to the inversion [10].

Both the Lorenz-Haken equations and its detuned version are special cases of Eqs. (2)–(4). When $\alpha = \theta = 0$, one readily obtains the standard Lorenz-Haken equations [10], and both x and y can be chosen to be real. A summary of the dynamical properties of this system can be found in a number of textbooks (see e.g. Ref. [10]).

When $\alpha = \theta \neq 0$, Eqs. (2)–(4) reduce to those describing a detuned two-level system. Indeed, by using the transformations $(\hat{x}, \hat{y}) = (x, y)\sqrt{1 + \alpha^2}\exp[i\alpha\sigma t/(\sigma + 1)]$ and $\hat{z} = z(1 + \alpha^2)$, we recover the equations for a detuned homogeneously broadened two-level system [12–14]:

$$\dot{\hat{x}} = -\sigma(1 - i\delta)\hat{x} + \sigma\hat{y}, \tag{5}$$

$$\dot{\hat{y}} = -(1 + i\delta)\hat{y} + (\hat{r} - \hat{z})\hat{x}, \tag{6}$$

$$\dot{\hat{z}} = -b\hat{z} + \mathrm{Re}(\hat{x}^*\hat{y}), \tag{7}$$

where the rescaled pump parameter $\hat{r}$ and the detuning δ are defined as:

$$\hat{r} \equiv r(1+\alpha^2), \quad \delta \equiv \frac{\alpha}{\sigma+1}. \tag{8}$$

The dynamical properties of Eqs. (5)–(7) have been investigated in Refs. [13,14]. There, in the bad-cavity case ($\sigma = 3, b = 1$) for detunings $\delta > 0.5$ only periodic solutions were found [14]. When $\alpha \neq \theta$, this scenario changes completely, as discussed in the next section. Interestingly, for detuned two-level systems $\hat{r}$ is the actual pump parameter, while for semiconductor lasers r should be used. This means that when a detuned two-level system shows interesting dynamics at some value $\hat{r}$, its semiconductor counter part (with $\alpha = \theta$) will show identical dynamics at a pump value reduced by a factor of $1+\alpha^2$.

3. Fixed points and their stability

In this section we analyze the fixed points and their stability for the generalized Lorenz-Haken equations (2)–(4).

3.1. First (lasing) threshold

Consider the trivial solution:

$$\mathrm{Re}(x_0) = \mathrm{Im}(x_0) = \mathrm{Re}(y_0) = \mathrm{Im}(y_0) = z_0 = 0, \tag{9}$$

which physically corresponds to the non-lasing state. Performing a linear stability analysis of the trivial solution is a standard technique to find the first threshold [10], i.e., the pump value at which the CW lasing action starts. By using this technique, the system determinant is found to be the following quadratic polynomial with complex coefficients:

$$D(s) = s^2 + (\sigma + 1 + i\theta)s + \sigma(1+i\theta)[1 - r(1 - i\alpha)]. \tag{10}$$

The characteristic equation, i.e., $D(s) = 0$, has a root with zero real part when the pump reaches the value:

$$r_{\mathrm{th},1} = \frac{-f + \sqrt{f^2 + g}}{2\sigma(\theta - \alpha)^2}, \tag{11}$$

where

$$f = (1+\alpha\theta)(\sigma+1)^2 - \theta(\sigma-1)(\theta-\alpha), \tag{12a}$$

$$g = 4\sigma(\theta-\alpha)^2\left[(\sigma+1)^2 + \theta^2\right]. \tag{12b}$$

Note that $r_{\mathrm{th},1}$ does not depend on b and that $r_{\mathrm{th},1}$ remains unchanged if α and θ simultaneously change sign. The singularity of Eq. (11) at $\theta = \alpha$ can cause numerical problems when α is too close to θ. These can be circumvented by employing the Taylor expansion of (11) up to first order in $(\theta - \alpha)$:

$$r_{\mathrm{th},1} = \frac{\alpha^2 + (\sigma+1)^2}{(1+\alpha^2)(\sigma+1)^2} + \alpha\sigma\frac{\alpha^2 - (\sigma+1)^2}{(1+\alpha^2)^2(\sigma+1)^3}(\theta-\alpha) + \mathcal{O}[(\theta-\alpha)^2]. \tag{13}$$

Thus, when $\theta = \alpha$, the first threshold reads, after using $\delta = \alpha/(\sigma+1)$:

$$r_{\mathrm{th},1} = \frac{1+\delta^2}{1+\alpha^2}, \quad \text{or } \hat{r}_{\mathrm{th},1} = 1+\delta^2, \tag{14}$$

which is in agreement with previous work [13,14].

Fig. 1 shows the influence of the two new parameters α and θ on the first threshold for $\sigma = 3$. Note the asymmetry caused by θ: For negative values of θ, the first threshold increases considerably, especially for large α. We only show positive α, since the first threshold is symmetric in simultaneous sign changes of α and θ. With increasing α, the first threshold decreases for positive θ, but it increases for negative θ. In Fig. 2 we show the location of the first threshold for a relatively small value of $\sigma = 1/30$ obtained by us-

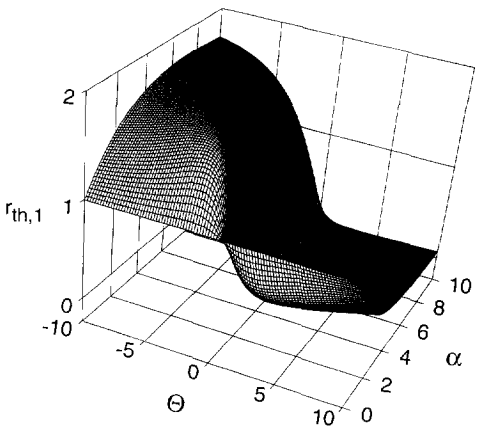

Fig. 1. First threshold as a function of α and θ when $\sigma = 3$.

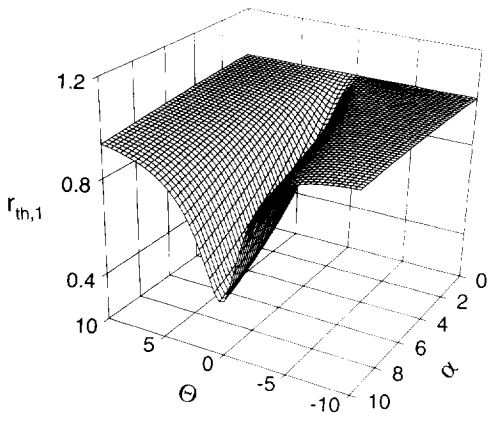

Fig. 2. First threshold as a function of α and θ when $\sigma = 1/30$. This value of σ corresponds to a single-mode bulk semiconductor laser.

ing typical semiconductor laser parameters ($\tau_P = 0.1$ ps and $\tau_E = 3$ ps). Note the dramatic difference with Fig. 1. Now, the absolute value of θ rather than its sign is relevant, while for increasing α, the first threshold decreases significantly only, when $|\theta|$ is smaller than ~ 2.5.

Obviously, reduction of the first threshold is very attractive from point of view of device design: the trend in the development of microlasers is directed towards the design of "thresholdless" lasers [15]. By controlling α or θ, one may realize substantial first threshold reduction. We will discuss the feasibility of this approach in Section 5.

3.2. Second (instability) threshold

We now find the location of the second threshold, i.e., the pump value at which the CW solution becomes unstable. Quite often, this is followed by a regime of self-pulsating behavior, indicative of a Hopf-bifurcation. The frequency involved in the bifurcation is a good estimate for the repetition rate of pulses. We will see that the two new parameters can have a dramatic effect on the value of the second threshold. Indeed, we find that in a large region of parameter space, where the resonant Lorenz-Haken system does not exhibit a second threshold, our generalized model does, leading to self-pulsations, period doubling, and possibly chaos. We first determine the steady-state (CW) solutions of the generalized equations (2)–(4). We write the CW solutions as:

$$x_s(t) = (a_s' + ia_s'')\exp(-i\Delta\omega_s t), \tag{15}$$

$$y_s(t) = (b_s' + ib_s'')\exp(-i\Delta\omega_s t), \tag{16}$$

$$z_s(t) = z_s, \tag{17}$$

where $a_s' + ia_s''$ and $b_s' + ib_s''$ are the respective complex amplitudes of the electric field and the polarization, and $\Delta\omega_s$ is a frequency shift with respect to ω_0. After substitution of Eqs. (15)–(17) into the generalized equations (2)–(4), it turns out that only the phase-difference between the electric field and polarization has a physical meaning. Therefore, without loss of generality we use

$$a_s' + ia_s'' = A_s\exp(i\varphi_s), \quad b_s'' = 0. \tag{18}$$

The phase difference φ_s is determined by

$$\sigma(\theta-\alpha)\tan^2\varphi_s - [(\sigma+1)(1+\alpha\theta)+\theta(\theta-\alpha)]\tan\varphi_s + \alpha(1+\theta^2) = 0, \tag{19}$$

whose solutions determine the other CW characteristics:

$$\Delta\omega_s = \sigma\tan\varphi_s, \tag{20a}$$

$$z_s = r - \left[(1+\alpha\theta)\cos^2\varphi_s - \tfrac{1}{2}(\theta-\alpha)\sin 2\varphi_s\right]^{-1}, \tag{20b}$$

$$A_s = \sqrt{bz_s}, \tag{20c}$$

$$a_s' = \pm A_s/\sqrt{1+(\Delta\omega_s/\sigma)^2}, \quad a_s'' = (\Delta\omega_s/\sigma)a_s', \tag{20d}$$

$$b_s' = \pm A_s\sqrt{1+(\Delta\omega_s/\sigma)^2}. \tag{20e}$$

When $\alpha = \theta$, Eq. (19) has only one solution, namely $\tan\varphi_s = \delta$, i.e., $\Delta\omega_s = \sigma\delta$, which explains the transformation used to obtain Eqs. (5)–(7). When $\alpha \neq \theta$, Eq. (19) has two solutions for $\tan\varphi_s$. When the laser is pumped above first threshold, only one of these solutions will have physical meaning; the other solution corresponds to an "anti-laser" state, where the inversion has a very high value (far above threshold) and hardly any power is generated. This is an unphysical state, and we will not consider this state in the remainder of the paper. It is noted that when pumped below first threshold, this "anti-laser" state becomes relevant when the system is subject to optical injection. In that

case, optical bistability can be found between the trivial state and the two "lasing" states [16]. In this paper we will only use pump levels that exceed the first threshold, so we only consider the single "normal" lasing solution, i.e., the CW solution with the inversion closest to threshold.

Each solution $\tan\varphi_s$ of Eq. (19) corresponds to one value for the inversion $r - z_s$ and field intensity $(a_s')^2 + (a_s'')^2$. The $\pm$ signs in Eqs. (20d), (20e) reflect the fact that when (x_s, y_s, z_s) is a solution of Eqs. (2)–(4), so is $(-x_s, -y_s, z_s)$. In the Lorenz-Haken model $\varphi_s = 0$, and the CW solution (19), (20a)–(20e) reduces to the well-known

$$\Delta\omega_s = 0, \quad z_s = r - 1, \tag{21a}$$

$$a_s' = b_s' = \pm\sqrt{b(r-1)}, \quad a_s'' = b_s'' = 0. \tag{21b}$$

The plus and minus signs in Eq. (21b) correspond to the two "eyes" of the Lorenz-attractor [10].

Performing a linear stability analysis around the fixed point determined by Eqs. (19)–(20e) yields the following quartic characteristic equation:

$$\sum_{j=0}^{4} d_j s^j = 0, \tag{22}$$

where the coefficients are given by

$$d_4 = 1, \tag{23a}$$

$$d_3 = 2(\sigma + 1) + b, \tag{23b}$$

$$d_2 = (\sigma+1)(\sigma+1+2b) + (\theta - 2\Delta\omega_s)^2 + \frac{bz_s}{r - z_s}\left[1 + \frac{\Delta\omega_s}{\sigma}(\theta - \Delta\omega_s)\right], \tag{23c}$$

$$d_1 = b(\sigma+1)^2 + b(\theta - 2\Delta\omega_s)^2 + \frac{bz_s}{r - z_s}\left[1 + 3\sigma + \theta^2 - \frac{\sigma - 1}{\sigma}\Delta\omega_s^2\right], \tag{23d}$$

$$d_0 = \frac{2bz_s}{r - z_s}\left[\sigma(\sigma+1) + \Delta\omega_s^2 + \sigma(\theta - \Delta\omega_s)^2\right]. \tag{23e}$$

Note that the stability of the lasing solution now also depends on the parameter b, in contrast with the stability of the trivial solution.

We look for the pump value at which the characteristic equation has a root of the form $s_{th,2} = i\Omega$ (zero real part). The frequency Ω can be a good indicator for the repetition rate of self-pulsations [17]. It should be noted that this frequency is not related to the frequency of relaxation oscillation, since that refers to the energy exchange between the field and the inversion only. In contrast, Ω is the angular frequency of the undamped energy exchange between field, inversion, and polarization. Without the active role of the polarization, there is no second threshold, as can easily be verified by analyzing the generalized equations after adiabatic elimination of the polarization.

From the characteristic equation, we obtain the following implicit equation for the second threshold:

$$\left(d_1^2 - d_1 d_2 d_3 + d_0 d_3^2\right)\Big|_{r=r_{th,2}} = 0, \tag{24}$$

and the frequency involved is given by $\Omega^2 = d_1/d_3$. The analytical form of $r_{th,2}$ from Eq. (24) is not easy to arrive at. In the simplest case, for which $\alpha = \theta = 0$, the second threshold becomes:

$$r_{th,2} = \sigma\left(\frac{\sigma + b + 3}{\sigma - b - 1}\right). \tag{25}$$

A necessary condition for (25) to have meaning is the aforementioned "bad-cavity condition" $\sigma > b+1$. For example, when $\sigma = 3$ and $b = 1$, the second threshold occurs at $r_{th,2} = 21$, but when $\sigma = 1/30$ and $b = 1/20000$ (typical values for a bulk semiconductor laser) no second threshold exists at all. For the detuned two-level system, Zeghlache and Mandel [14] derived a power series in the detuning δ for the second threshold $\hat{r}_{th,2}(\delta)$. It is interesting to note that, whereas for all δ $\hat{r}_{th,2}(\delta) > \hat{r}_{th,2}(0)$ (detuning shifts the second threshold to higher values), the opposite is true for $r_{th,2}(\delta)$ (without the hat) in a large region in (α, θ)-space. The cause for this is the asymmetry parameter α, which effectively reduces the second threshold. It is a well-known fact that inhomogeneously broadened systems have a lower second threshold than their homogeneously broadened counterparts [8].

We now illustrate the behavior of the second threshold as a function of α and θ by solving Eq. (24) for two combinations of σ and b.

To study a system that satisfies the bad-cavity condition, we take $\sigma = 3$ and $b = 1$. Fig. 3 shows the second threshold $r_{th,2}(\alpha, \theta)$ scaled to its Lorenz-Haken value $r_{LH} \equiv r_{th,2}(0,0) = 21$. Again we only show positive α since the characteristic equation remains unchanged under simultaneous sign-changes of α and θ. Around

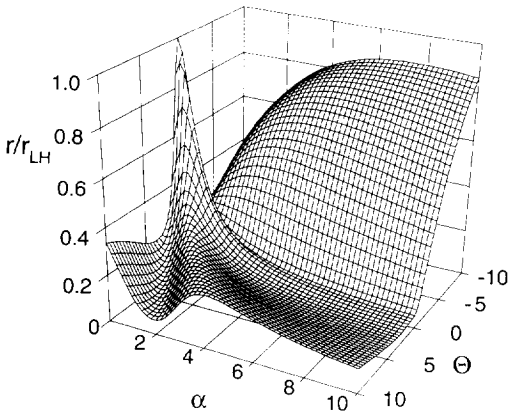

Fig. 3. Second threshold as a function of α and θ, when $\sigma = 3$ and $b = 1$, normalized to the Lorenz-Haken value $r_{th,2}(\alpha = 0, \theta = 0) = 21$. The bad-cavity condition is satisfied for these parameters.

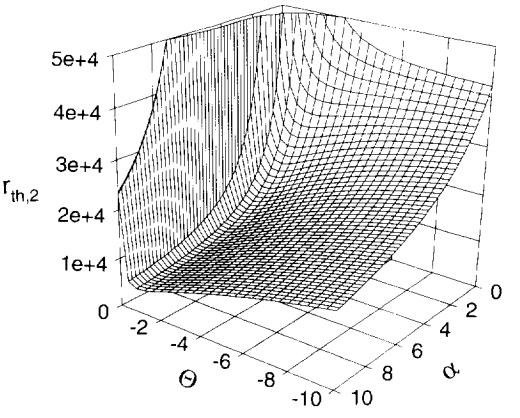

Fig. 4. Second threshold as a function of α and θ when $\sigma = 1/30$ and $b = 1/20000$, typical values for single-mode bulk semiconductor lasers. The bad-cavity condition is not satisfied for these parameters.

$(\alpha = 0, \theta = 0)$ a sharp peak in $r_{th,2}$ is found, corresponding to the resonant Lorenz-Haken case. Starting at the peak, $r_{th,2}$ first decreases in all directions. Then, depending on the direction, more complicated behavior is found. Note that negative values of θ are accompanied by an increasing second threshold. For positive values of both θ and α a dramatic reduction can be achieved. This is in agreement with the behavior of the first threshold: in Fig. 1 the first threshold is also dramatically reduced for positive θ.

When a system does not satisfy the bad-cavity condition the results are even more surprising. When $\sigma = 1/30$ and $b = 1/20000$ (typical values for bulk semiconductor lasers: $\tau_P = 0.1$ ps, $\tau_E = 3$ ps, and $\tau_N = 2$ ns), the two additional degrees of freedom α and θ allow for a second threshold in a large region of parameter space (see Fig. 4). Note that now, in contrast with the bad-cavity case (Fig. 2), positive θ increases the second threshold. The fact that the values of the second threshold are relatively large is less important than that the second threshold exists at all. By increasing σ and b, these high values decrease to more useful ones. The main point to note is that the bad-cavity condition is no longer a prerequisite for the second threshold to exist. In Section 5, we will discuss the possibilities to decrease the second threshold to a more accessible value.

4. Laser dynamics beyond the second threshold

So far we described the effect of two new parameters, that take the asymmetry of the inhomogeneously broadened gain profile into account, on the position of both first and second laser threshold. To illustrate the effect of α and θ on the laser dynamics beyond the second threshold, we have numerically solved the generalized equations (2)–(4) for four combinations of α and θ for a laser satisfying the bad-cavity condition ($\sigma = 3$ and $b = 1$) while operating at $r = 2r_{th,2}$. Fig. 5 shows the laser-intensity dynamics for the four combinations. In each case, we show on the left the trajectory of the system projected on the $|x|^2$–$|y|^2$ phase space, and on the right a sample of the associated laser-intensity evolution. The values of α and θ as well as $r_{th,2}$ are given in the figure. For reference, we show in Fig. 5(a) the situation for the resonant Lorenz-Haken model, i.e., with both α and θ equal to zero and $r_{th,2} = 21$. Pumped at $r = 2r_{th,2}$, the system exhibits the well-known Lorenz chaos. In Figs. 5(b)–(d) we show the effect of nonzero α (b), nonzero θ (c), and both α and θ nonzero (d). Note the striking change on the dynamics for relatively small values of α and θ. The electric-field intensity is periodic in all three cases, a feature similar to that of the detuned ($\delta > 0.5$) two-level system, where it was concluded that the introduction of a detuning destroys much of the complicated behavior of the Lorenz-Haken equations and has a definite stabilizing effect [14].

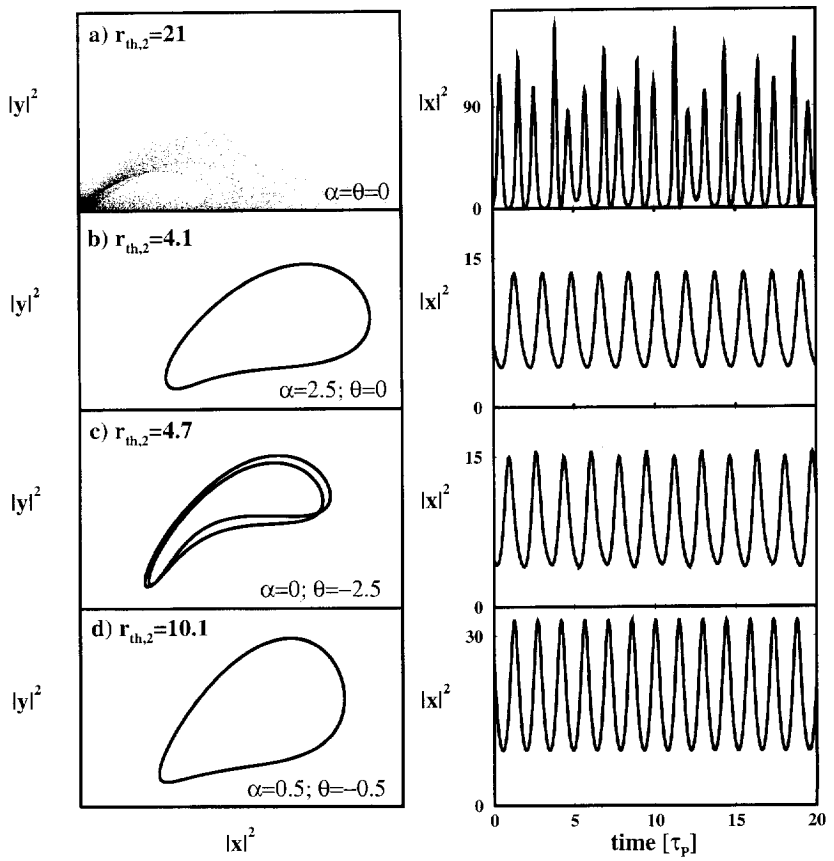

Fig. 5. Laser intensity dynamics of a bad-cavity laser for four different combinations of α and θ, but all operated at $r = 2r_{th,2}$. Parameters are: $\sigma = 3$, $b = 1$. For each combination we show on the left-hand-side the trajectory of the system projected on the $|x|^2$–$|y|^2$ phase space, while the right-hand-side shows a sample of the corresponding evolution of the laser field intensity $|x|^2$. (a) $\alpha = \theta = 0$, $r_{th,2} = 21$, "classical" Lorenz-Haken chaos; (b) $\alpha = 2.5$, $\theta = 0$, $r_{th,2} = 4.1$, periodic modulation; (c) $\alpha = 0$, $\theta = -2.5$, $r_{th,2} = 4.7$, period-2; (d) $\alpha = 0.5$, $\theta = -0.5$, $r_{th,2} = 10.1$, periodic.

Note, however, the period-2 dynamics in case (c) for a negative value of θ. The intensity evolution seen in Fig. 5 does not convey all information since phase dynamics is lost. For this reason, we have chosen to look at the evolution of the real parts of the complex electric field amplitude and the induced polarization. Indeed, as seen in Fig. 6, a different picture emerges. On the left side of Fig. 6, we plot the trajectory of the system projected on the $\mathrm{Re}(x)$–$\mathrm{Re}(y)$ phase space, and on the right a sample of the associated time-trace of the real part of the electric field amplitude. Since the phase of the laser field is irrelevant in the Lorenz-Haken case, no additional information is obtained from Fig. 6a. In the other three cases (a,b,c), however, the phase does play an important role, and we find phase dynamics qualitatively similar to the Lorenz-Haken case (a), although the attractor is quite different in each case. It appears that although the intensity dynamics is much simplified by the introduction of the "detuning" parameter θ and the asymmetry parameter α, the phase dynamics remains chaotic.

5. Discussion: applications of the model

After Lorenz' famous paper on Rayleigh-Bénard convective fluid dynamics as a model for the unpredictability of atmospheric turbulence, in which a first-order approximation resulted in the Lorenz-equations, it took more than a decade before it was realized by

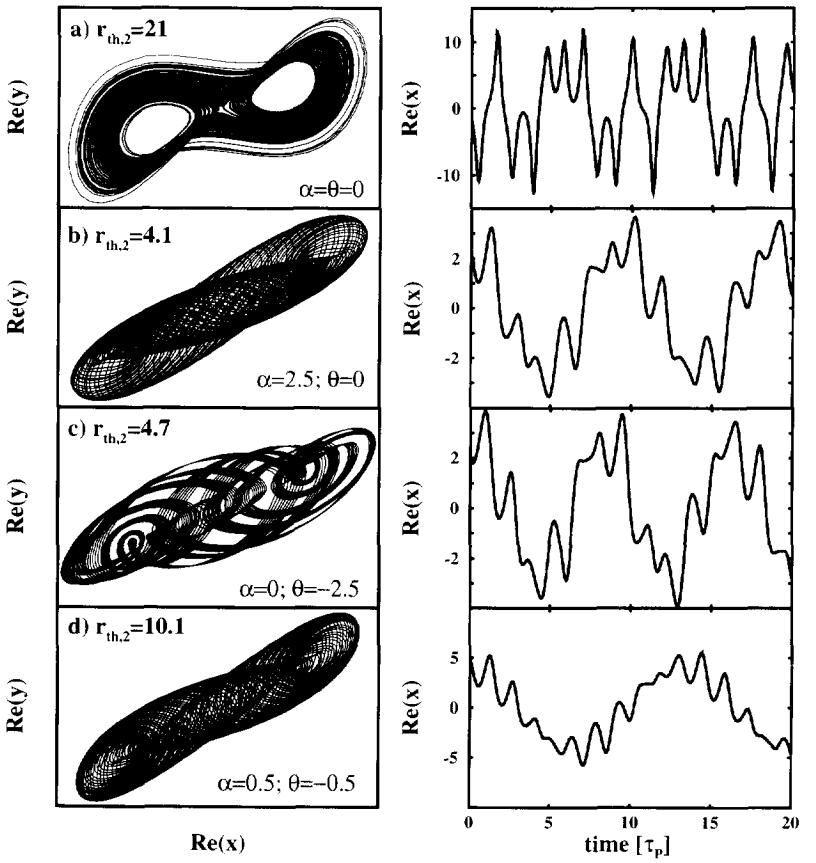

Fig. 6. Same as Fig. 5, except now the real parts of the electric field and the induced polarization are shown. Phase dynamics lost in Fig. 5 is retained here.

Haken that the same equations also describe a homogeneously broadened two-level system [1,2]. This shows that one cannot predict in what context a specific nonlinear dynamics model will be used. In fact, it may very well be that our generalized Lorenz-Haken equations find use in both fluid dynamics and nonlinear optics (or indeed in any other branch of nonlinear science).

Here, we focus on the applicability of our model to single-mode semiconductor lasers. The most complete description of the semiconductor gain medium is in the form of microscopic semiconductor Bloch-equations, requiring fairly large computational effort to be solved [18]. In the last few years, a number of papers have appeared that attempt to model the material polarization in a macroscopic manner [19–21]. Naturally, all formulations have in common that the microscopic equations are averaged over the density of states. When doing so, one is confronted with the impossibility of getting a closed form for the time dependence of the macroscopic material polarization. Instead, a hierarchy of equations for the microscopic dipole moment is obtained. One way to deal with such an infinite hierarchy was put forward by Graham and Cho [8] in the case of inhomogeneously broadened gas-lasers.

A similar approach for single-mode semiconductor lasers was used by Yao et al. [9], who proposed a different truncation of the hierarchy, yielding two additional variables, called κ and ζ. The quantity κ measures the carrier-induced complex gain (optical gain and refractive index), while ζ accounts for the dipole-induced complex change of the macroscopic polarization decay rate. The resulting model is in a sense

"mesoscopic": the two new (complex) variables are time-independent in the macroscopic equations, but need to be determined self-consistently from the microscopic equations. Our generalized Lorenz-Haken equations are a rescaled version of the macroscopic equations of Ref. [9].

It was found in Ref. [9] that κ varies little with the carrier density N around threshold, while to a good approximation ζ varies linearly with N in the range over which N is likely to vary in most semiconductor lasers ($1\times10^{18}\,\mathrm{cm}^{-3} < N < 3\times10^{18}\,\mathrm{cm}^{-3}$). A linear variation of ζ (although called differently) was also used in Ref. [21] where semiconductor lasers are described as an effective two-level model with three additional parameters. Theoretical expressions that prescribe how the additional parameters must be calculated from the microscopic theory and how they are interrelated, were not given in Ref. [21]. The relation between κ and ζ and the two new parameters α and θ in Eqs. (2)–(4) is given by

$$\kappa = \mathrm{Re}(\kappa)(1 - i\alpha), \tag{26}$$

$$\zeta = \mathrm{Re}(\zeta)(1 + i\theta). \tag{27}$$

Here, α is the well-known linewidth enhancement factor [11]. The parameter θ has its origin in the fact that averaging over the band energies makes the effective polarization decay rate complex. Therefore, θ must be interpreted as an effective detuning for an inhomogeneously broadened system. For the sake of completeness, all relevant expressions from Ref. [9] are given in the Appendix.

Because of the self-consistency requirement, both κ and ζ (and therefore α and θ) are in principle time-dependent, through the carrier density. When the semiconductor laser is operating in CW mode (below the second threshold), one can generally ignore this time-dependence: using selfconsistent values of α and θ is sufficient. Strictly speaking, the dynamics of the two quantities should be taken into account when the linear stability analysis is performed. This dynamics can be readily neglected, when the carrier decay rate b is much smaller than the photon decay rate σ [9]. Of course, when the system is pumped above the second threshold, the dynamics of α and especially θ may not be neglected. It is with this in mind that we will apply our model on single-mode semiconductor lasers.

Table 1
First and second threshold for typical bulk and QW single-mode semiconductor lasers by using parameters from Ref. [9]

Type	σ^{-1}	b^{-1}	α	θ	$r_{\mathrm{th},1}$	$r_{\mathrm{th},2}$
Bulk	30	20000	5	−5	1.001	15823
QW	60	40000	2	−1.6	0.997	37262

In Table 1, we give the values of σ, b, α, θ, and the first and second threshold for typical single-mode bulk and quantum-well semiconductor lasers, using the results of Ref. [9]. Note that the carrier decay rate b is much smaller than the photon decay rate σ, justifying the neglect of the microscopic dynamics of α and θ. Although there exists a second threshold for both types of lasers, which is not predicted by the "classical" Lorenz-Haken model, the values are too high to be of practical interest.

One may explore the possibilities to get a semiconductor laser to exhibit a second threshold around $r = 10$, while keeping both α and θ fixed at their original values (for a bulk semiconductor laser $\alpha = 5$ and $\theta = -5$). We have found, that in order to achieve this, both σ and b have to be increased substantially. Although τ_{P} may be increased somewhat by operating at low temperatures (to reduce the contribution of phonons), a substantial increase does not appear to be likely. Decreasing the carrier lifetime and the photon lifetime simultaneously will also have the desired effect. The photon lifetime τ_{ph} can be decreased by antireflection coating and values below 1 ps are feasible. The carrier relaxation time can be reduced using some recent techniques [23] and values in the range 0.3 ps $< \tau_{\mathrm{N}} <$ 3 ns are feasible. In Figs. 7 and 8 we show the intensity and (complex) amplitude dynamics of a quantum-well semiconductor laser pumped at four different values above the second threshold, occurring at $r_{\mathrm{th},2} = 8.9$ for the relaxation times $\tau_{\mathrm{ph}} = 167$ fs, $\tau_{\mathrm{P}} = 100$ fs, and $\tau_{\mathrm{N}} = 500$ fs, while $\alpha = 2$ and $\theta = -1.6$.

At $r = 1.05 r_{\mathrm{th},2} \approx 10 r_{\mathrm{th},1}$ (Fig. 7a), the intensity shows an almost perfect harmonic modulation. As the pump increases, the periodic modulation becomes more anharmonic for $r = 1.15 r_{\mathrm{th},2}$ (Fig. 7b), exhibits period doubling at $r = 1.2 r_{\mathrm{th},2}$ (Fig. 7c), and evolves towards quasi-periodic behavior when $r = 1.235 r_{\mathrm{th},2}$ (Fig. 7d). In cases (a) and (b), the contrast of the intensity modulation is quite good, and the quantum-

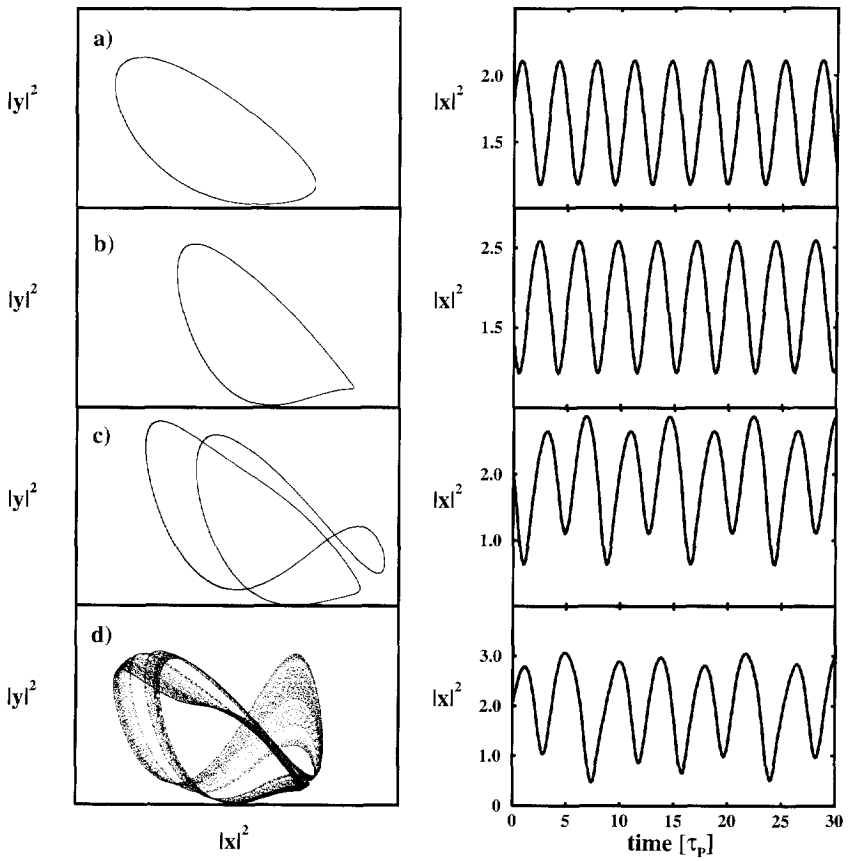

Fig. 7. Laser intensity dynamics of a modified (τ_E = 300 fs and τ_N = 500 fs) quantum-well laser at at four different pumps, when the microscopic dynamics of α and θ is neglected. Parameters are: $\sigma = 0.3$, $b = 0.2$, $\alpha = 2$, and $\theta = -1.6$. The first threshold is located at $r_{th,1} = 1.006$ while the second threshold is found at $r_{th,2} = 8.9$. Left-hand-side depicts the trajectory of the system projected on the $|x|^2$–$|y|^2$ phase space, while the right-hand-side shows a sample of the corresponding evolution of the laser intensity $|x|^2$. (a) $r = 1.05r_{th,2}$, harmonic modulation; (b) $r = 1.15r_{th,2}$, slightly anharmonic modulation; (c) $r = 1.2r_{th,2}$, period-2 behavior; (d) $r = 1.235r_{th,2}$, quasi-periodic behavior.

well laser may serve as a self-pulsing laser at a repetition rate $\sim$ 2 THz.

As in the case of the bad-cavity laser (Figs. 5 and 6), the intensity evolution in Fig. 7 does not convey all information. Fig. 8 shows the corresponding phase dynamics of the field amplitude and induced polarization. The frequency of the intensity modulation, which remains roughly the same for increasing pump, is retained in the phase dynamics, and is on the order of $0.3/\tau_P$.

Fig. 8 shows, however, an additional oscillation, whose frequency increases from $\sim 0.003/\tau_P$ in Fig. 8a to $\sim 0.03/\tau_P$ in Fig. 8d. This slow oscillation is the well-known semiconductor laser relaxation oscillation. As the pump increases, the relaxation oscillation frequency approaches the fast frequency, and their interaction becomes observable at $r = 1.20r_{th,2}$ (Fig. 8c). When $r = 1.235r_{th,2}$ (Fig. 8d), the phase is fully chaotic due to this frequency mixing.

It should be realized, however, that the parameters used to obtain Figs. 7 and 8 barely justify neglecting the dynamics of α and θ. A full analysis, however, goes beyond the scope of this paper.

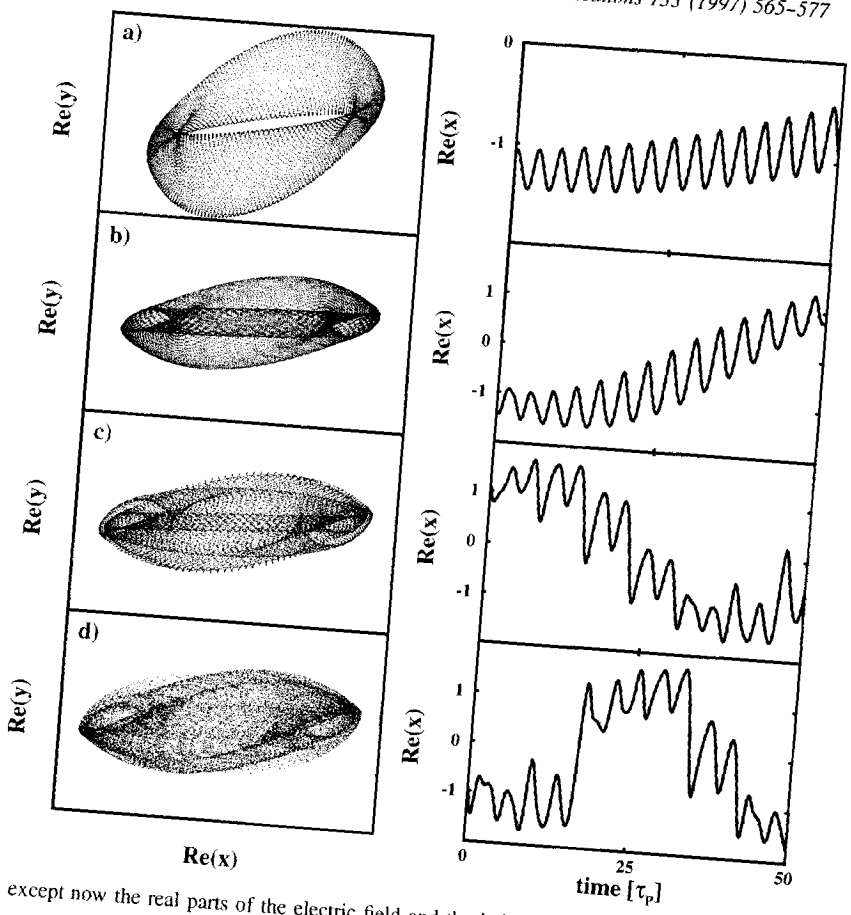

Fig. 8. Same as Fig. 7, except now the real parts of the electric field and the induced polarization are shown. Phase dynamics lost in Fig. 7 is retained here.

6. Conclusions

We have presented a new set of equations which serve as a generalization of the Lorenz-Haken equations, both for the resonant and the detuned case. Apart from the standard parameters σ (ratio of dipole lifetime and twice the photon lifetime) and b (ratio of dipole lifetime and carrier lifetime), two additional parameters α and θ account for the asymmetry of the gain and inhomogeneous broadening. When α and θ are zero, the model reduces to the resonant Lorenz-Haken case. When chosen equal but not zero, the equations describe a detuned two-level system. The effect of these new parameters on the location of the first (lasing) threshold and the second (instability) threshold is investigated. It is found that the first threshold is greatly reduced when α and θ have opposite sign. The second threshold is heavily dependent on the values of α and θ. However, because of them, the laser need not satisfy the so-called bad-cavity condition to have a second threshold.

Examples of dynamic evolution beyond the second threshold are given for various values of α and θ. Similar to the case of the detuned, homogeneously broadened, two-level system, we find that the intensity dynamics is stabilized by the introduction of the two new parameters. However, the phase shows rich nonlinear dynamics. As a result, a self-pulsating laser (periodic evolution of the laser intensity) may still exhibit phase chaos.

These generalized Lorenz-Haken equations are a rescaled form of a recently reported macroscopic model for ultrafast semiconductor laser dynamics. Our model predicts, for the first time to our knowl-

edge, that single-mode semiconductor lasers can exhibit a second threshold, even though they do not satisfy the bad-cavity condition. For typical semiconductor lasers the second threshold is too high for any practical purposes. However, the second threshold is reduced significantly when both the photon- and the carrier-lifetimes are shorter. In that case our model is close to the limit where, in the case of semiconductor lasers, the dynamics of α and θ may no longer be neglected, but may be applicable to other nonlinear (optical) systems.

Acknowledgements

The research of GHMvT is made possible through a grant from the Netherlands Organization of Scientific Research (NWO). This work is also supported by the U.S. Army Research Office.

Appendix A

In Ref. [9], an effective Maxwell-Bloch description is given for a single-mode semiconductor laser. The microscopic Bloch equations for the occupation probabilities n_e (electrons) and n_h (holes) and the transition probability p need to be averaged over the density of states in the semiconductor bands to yield equations for the macroscopic carrier density N and polarization P. By defining two complex quantities κ and ζ as

$$\kappa N = \left\langle \frac{n_e + n_h - 1}{1 + i\Delta} \right\rangle, \tag{A.1}$$

$$\zeta = \left(\frac{P}{2\mu} \right) \Big/ \left\langle \frac{p}{1 + i\Delta} \right\rangle, \tag{A.2}$$

where μ is the dipole moment and $\Delta = (\omega - \omega_0)\tau_{in}$ is the detuning between an individual resonance and the optical frequency scaled to the dipole dephasing time τ_{in}, the following macroscopic Maxwell-Bloch equations are obtained:

$$\frac{dE}{dt} = \frac{i\omega_0}{2nn_g\epsilon_0} P - \frac{1}{2\tau_{ph}} E, \tag{A.3}$$

$$\frac{dP}{dt} = -\zeta \left(\frac{P}{\tau_{in}} + i\kappa \frac{\mu^2}{\hbar} EN \right), \tag{A.4}$$

$$\frac{dN}{dt} = \frac{I}{qV} - \frac{N}{\tau_{el}} + \frac{1}{2\hbar} \operatorname{Im}\left(E^* P\right). \tag{A.5}$$

Here, E is the complex electric field amplitude, τ_{ph} is the photon lifetime, τ_{el} is the carrier relaxation time, and I is the pump current density. Further, ω_0 is the optical frequency, n is the background refractive index, n_g is the group index, q is the elementary charge, and V is the active volume.

Upon inspection of (A.4) one finds that by averaging the individual transitions (with dephasing time τ_{in}) over the asymmetric bands, the effective two-level dephasing time and detuning are $\tau_P = \tau_{in}/\mathrm{Re}(\zeta)$ and $\Delta_{eff} = \mathrm{Im}(\zeta)/\tau_{in}$, respectively.

By normalizing time to τ_P and using (26), (27), and the following definitions:

$$x \equiv \sqrt{\frac{nn_g\epsilon_0\tau_P}{\hbar\omega_0 N_{th}\tau_E}}\, E, \tag{A.6a}$$

$$y \equiv i\omega_0 \sqrt{\frac{\tau_P\tau_E}{4\hbar\omega_0 nn_g\epsilon_0 N_{th}}}\, P, \tag{A.6b}$$

$$z \equiv r - (N/N_{th}), \tag{A.6c}$$

$$N_{th} \equiv \frac{2\hbar\epsilon_0 nn_g}{\mathrm{Re}(\kappa)\omega_0\tau_E\tau_{in}\mu^2}, \tag{A.6d}$$

$$r \equiv I\tau_N/(qVN_{th}), \tag{A.6e}$$

the generalized Lorenz-Haken equations (2)–(4) are obtained from Eqs. (A.3)–(A.5).

References

[1] E.N. Lorenz, J. Atmos. Sci. 20 (1963) 130.
[2] H. Haken, Phys. Lett. A 53 (1975) 77.
[3] F.T. Arecchi, G.L. Lippi, G.P. Puccioni and J.R. Tredicce, Coherence and Quantum Optics V, Eds. J.H. Eberly, L. Mandel and E. Wolf (Plenum, New York, 1984), 1227.
[4] J.R. Tredicce, F.T. Arecchi, G.L. Lippi, and G.P. Puccioni, J. Opt. Soc. Am. B 2 (1985) 173.
[5] For a recent review on semiconductor lasers with optical injection and feedback, see: G.H.M. van Tartwijk and D. Lenstra, Quantum Semiclass. Opt. 7 (1995) 87.
[6] G.H.M. van Tartwijk, A.M. Levine and D. Lenstra, IEEE J. Sel. Top. Quantum Electron. 1 (1995) 466.
[7] I. Fischer, G.H.M. van Tartwijk, A.M. Levine, W.E. Elsässer, E.O. Göbel and D. Lenstra, Phys. Rev. Lett. 76 (1996) 200.
[8] R. Graham and Y. Cho, Optics Comm. 47 (1983) 52.
[9] J. Yao, G.P. Agrawal, P. Gallion and C.M. Bowden, Optics Comm. 119 (1995) 246.
[10] C.O. Weiss and R. Vilaseca, Dynamics of Lasers (VCH, Weinheim, 1991).

[11] C.H. Henry, IEEE J. Quantum Electron. QE-18 (1982) 259.
[12] H. Risken, C. Schmid and W. Weidlich, Z. Phys. 194 (1966) 337.
[13] P. Mandel and H. Zeghlache, Optics Comm. 47 (1983) 146.
[14] H. Zeghlache and P. Mandel, J. Opt. Soc. Am. B 2 (1985) 18.
[15] F. De Martini, F. Cairo, P. Mataloni and F. Verzegnassi, Phys. Rev. A 46 (1992) 4220.
[16] G.H.M. van Tartwijk, H. De Waardt, B.H. Verbeek and D. Lenstra, IEEE J. Quantum Electron. 30 (1994) 1763.
[17] G.H.M. van Tartwijk and M. San Miguel, IEEE J. Quantum Electron. 32 (1996) 1191.
[18] H. Haug and S.W. Koch, Quantum Theory of Optical and Electronic Properties of Semiconductors (World Scientific, Singapore, 1990).
[19] C.M. Bowden and G.P. Agrawal, Optics Comm. 100 (1993) 147.
[20] C.M. Bowden and G.P. Agrawal, Phys. Rev. A 51 (1995) 4132.
[21] S. Balle, Optics Comm. 119 (1995) 227.
[22] G.P. Agrawal and C.M. Bowden, IEEE Photon. Technol. Lett. 5 (1993) 640.
[23] W.J. Schaff, S.D. Offsey, X.J. Song, L.F. Eastman, T.B. Norris, W.I. Sha and G.A. Mourou, Proc. MRS Symp. 241 (1992) 51–62.